

THE CKM PARADIGM: IMPLICATIONS OF THE MOST RECENT RESULTS

SANDRINE LAPLACE

Laboratoire de l'Accélérateur Linéaire, IN2P3-CNRS et Université Paris-Sud, BP 34, F-91898 Orsay Cedex, FRANCE

The implications of the most recent experimental results in the B and K meson systems on the CKM paradigm are investigated by means of a global fit to the theoretical predictions of the Standard Model. We advocate the frequentist approach *Rfit*, which is implemented in the *CKMfitter* package. Within this approach, constraints on the CKM parameters and other quantities of interest are obtained, and extensions of the Standard Model are investigated.

LAL 02-79

1 Introduction

The electroweak sector of the Standard Model (SM) has been intensively studied during the last decades, in particular at LEP and SLD. CP violation in flavour changing processes is the next sector to be investigated. CP violation was first observed in the Kaon system¹, and recently established in the B -meson system², but within the SM it cannot produce a baryon asymmetry as large as what is observed in the universe³. A variety of models beyond the SM introduce new sources of CP violation: therefore, CP violation is an interesting place to look for new physics, and particularly in the B -meson system where there are numerous large CP -violating observables.

Within the Standard Model, CP violation is accounted for by one phase^a in the CKM matrix^{5,6} which describes the charged current couplings among left-handed quark fields. With three generations, the CKM matrix is parameterized by four parameters (including the CP violating phase). We use the Wolfenstein parameterization⁷, which, following the observed hierarchy between the matrix elements, expands the CKM matrix in terms of the four parameters ρ , η , A and λ ($\lambda \simeq 0.22$ being the expansion parameter). Presently, λ is known at the 1% level, A at the 5% level, whereas ρ and η are the least known CKM parameters. Many relations between the matrix elements follow from the unitarity of the CKM matrix. In particular, the unitarity relation linking the first and third rows of the matrix is usually displayed as the Unitarity Triangle (UT) in the complex plane $(\bar{\rho}, \bar{\eta})$ ^b.

Investigating the charged current couplings among quarks is not a straightforward task since quarks also (and mainly) undergo the strong interaction, in which calculations are not always accurate. Therefore, the SM prediction of many CKM observables suffers from uncertainties arising from the use of approximations in QCD computations. These hard-to-quantify uncertainties do not belong to the well-defined framework of Gaussian statistics.

^aWith more than three generations, there would be more CP violating phases.

^bThe replacements $\rho \rightarrow \bar{\rho} = \rho(1 - \lambda^2/2)$ and $\eta \rightarrow \bar{\eta} = \eta(1 - \lambda^2/2)$ improves the accuracy of the UT apex.

In order to avoid drawing wrong conclusions from the global CKM fit of such observables, one needs a robust and sufficiently conservative approach: we advocate the frequentist approach *Rfit*⁸, within the framework of the *CKMfitter* package, and describe its main features and results in the following.

2 Statistical Framework and Fit Ingredients

In the *Rfit* frequentist statistical framework, theoretical uncertainties are treated without *a priori* knowledge except for the definition of ranges^{9,10}. In particular, no probability distribution functions are considered¹¹. Practically, the fit likelihood is the product of an experimental part, $\mathcal{L}_{\text{exp}}(x_{\text{exp}} - x_{\text{theo}}(y_{\text{mod}}))$ comparing the measurements x_{exp} to the theoretical predictions x_{theo} (the latter depending on some model parameters y_{mod})^c, with a theoretical part, $\mathcal{L}_{\text{theo}}(y_{\text{QCD}})$ ^d which describes our knowledge on the QCD parameters $y_{\text{QCD}} \in y_{\text{mod}}$. A pseudo- χ^2 is built as $\chi^2 = -2\ln\mathcal{L}$ and is minimized in the fit.

The analysis is divided into three steps: first, the overall consistency between data and the theoretical framework (here, the SM) is tested by means of a Monte Carlo simulation. If the agreement between data and the SM is found to be acceptable, confidence levels (CL) in parameter subspaces are determined (*e.g.*, in the $\bar{\rho}-\bar{\eta}$ plane). Finally, extensions of the SM can be tested and limits on new physics parameters are determined.

Table 1 gives the input ingredients of the fit. For $|V_{ub}|$, the inclusive measurement of LEP¹² and exclusive measurement of CLEO¹³ have been used, as well as the inclusive CLEO analysis using the $B \rightarrow X_s \gamma$ spectrum¹⁴. The input to the fit is the product of these three measurement likelihoods. The inclusive and exclusive LEP and CLEO $|V_{cb}|$ measurements are averaged before entering the fit¹⁵. For Δm_s , we translate the preferred value of the amplitude spectrum¹⁶ into a confidence level curve¹⁷. Finally, we use the world average of $\sin 2\beta$, dominated by the measurements of *BABAR* and *Belle*².

3 Standard Fit

The consistency between data and the SM is gauged by the value of the overall minimum χ^2 , from which a CL is inferred by means of a Monte Carlo simulation. Many sets of measurements are generated following the experimental likelihood distribution in which the theoretical predictions are computed for the best fitted values of the theoretical parameters. A fit is then performed on each of these sets, varying all the model parameters freely, and the CL of the SM fit is assigned by integrating the χ^2 distribution thus obtained, up to the overall minimum χ^2 .

Figure 1 shows the distribution of the Monte Carlo generated χ^2 (histogram), and the associated CL (smooth curve). The arrow shows the χ^2 of the standard fit, corresponding to a CL of 57%. The agreement between data and Standard Model is thus excellent, and we assign CL to various parameters of interest: Fig. 2 displays CL in the $(\bar{\rho}-\bar{\eta})$ plane. For the individual constraints are shown the regions inside which $CL \geq 5\%$, including the 4-fold ambiguity from the $\sin 2\beta$ measurement. The latter is in perfect agreement with the SM prediction, demonstrating that the CKM mechanism is the dominant source of *CP* violation in flavour changing processes at the electroweak scale.

^cThe four CKM parameters are part of these model parameters.

^dA range of y_{QCD} is obtained from QCD theoretical calculations: $\mathcal{L}_{\text{theo}}(y_{\text{QCD}})=1$ for y_{QCD} inside the range, and 0 when outside.

Table 1: Input observables and parameters for the global CKM fit. When two errors are quoted, the first one is statistical and the second one systematic. When one error is quoted, it is statistical unless stated otherwise.

Parameter	Value \pm Error(s)
$ V_{ud} $	0.97394 ± 0.00089
$ V_{us} $	0.2200 ± 0.0025
$ V_{ub} $ (LEP incl.) ¹²	$(4.08 \pm 0.61 \pm 0.47) \times 10^{-3}$
$ V_{ub} $ (CLEO incl.) ¹⁴	$(4.08 \pm 0.56 \pm 0.40) \times 10^{-3}$
$ V_{ub} $ (CLEO excl.) ¹³	$(3.25 \pm 0.29 \pm 0.55) \times 10^{-3}$
$ V_{cd} $	0.224 ± 0.014
$ V_{cs} $	0.969 ± 0.058
$ V_{cb} $ ¹⁵	$(40.4 \pm 1.3 \pm 0.9) \times 10^{-3}$
$ \epsilon_K $	$(2.271 \pm 0.017) \times 10^{-3}$
Δm_d ¹⁶	$(0.496 \pm 0.007) \text{ ps}^{-1}$
Δm_s ¹⁶	See Text
$\sin 2\beta_{\text{WA}}$ ²	0.780 ± 0.077
m_c	$(1.3 \pm 0.1_{\text{sys}}) \text{ GeV}$
$m_t(\overline{\text{MS}})$	$(166.0 \pm 5.0) \text{ GeV}$
m_K	$(493.677 \pm 0.016) \text{ MeV}$
Δm_K	$(3.4885 \pm 0.0008) \times 10^{-15} \text{ GeV}$
m_{B_d}	$(5.2794 \pm 0.0005) \text{ GeV}$
m_{B_s}	$(5.3696 \pm 0.0024) \text{ GeV}$
m_W	$(80.419 \pm 0.056) \text{ GeV}$
G_F	$(1.16639 \pm 0.00001) \times 10^{-5} \text{ GeV}^{-2}$
f_K	$(159.8 \pm 1.5) \text{ MeV}$
B_K	$0.87 \pm 0.06 \pm 0.13$
η_{cc}	$1.38 \pm 0.53_{\text{sys}}$
η_{ct}	$0.47 \pm 0.04_{\text{sys}}$
η_{tt}	$0.574 \pm 0.004_{\text{sys}}$
$\eta_B(\overline{\text{MS}})$	$0.55 \pm 0.01_{\text{sys}}$
$f_{B_d} \sqrt{B_d}$	$(230 \pm 28 \pm 28) \text{ MeV}$
ξ	$1.16 \pm 0.03 \pm 0.05$

4 Beyond the Standard Fit

4.1 Rare K Decays

The detection of a second $K^+ \rightarrow \pi^+ \nu \bar{\nu}$ event was announced early 2002 by the E787 Collaboration at Brookhaven¹⁸, leading to a branching ratio of $(1.57^{+1.75}_{-0.82}) \times 10^{-10}$ which is compatible with the SM prediction¹⁹ given in Table 2. A total of 5 to 10 SM events is expected to be detected at the successor experiment E949 at BNL²⁰, and thus this channel will become an important ingredient of the CKM fits.

4.2 Charmless B Decays

Both the α and γ angles of the UT can in principle be extracted from the charmless two-body decays $B \rightarrow \pi\pi$ and $B \rightarrow K\pi$, for which the data start to accumulate. Therefore, a lot of effort^{21,22} has been put recently in the calculation of the charmless two-body hadronic matrix elements using the factorization concept.

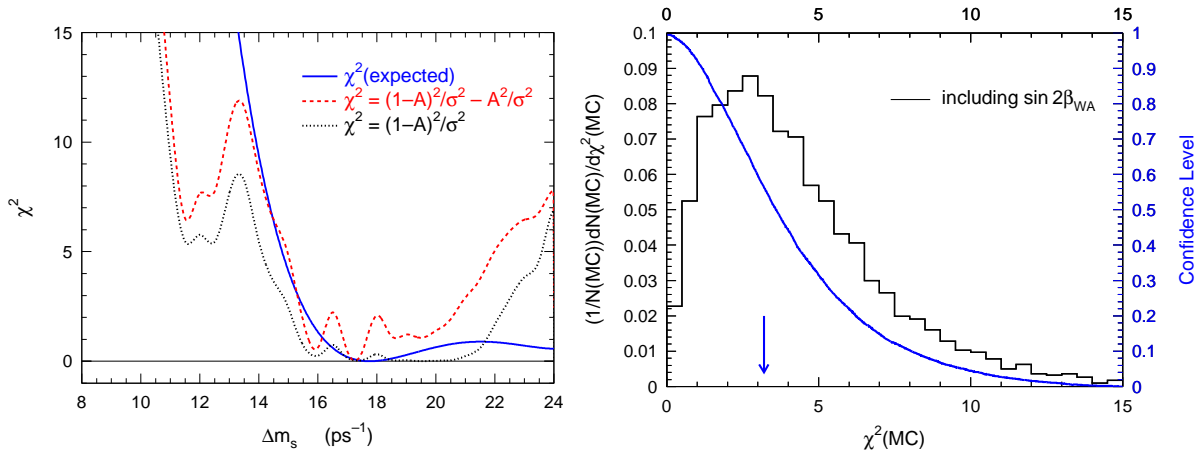


Figure 1: Left figure: χ^2 curves for various interpretations of the amplitude spectrum of Δm_s : the modified amplitude method⁸ (dotted line), the likelihood ratio method¹¹ (dash-dotted line), the expected χ^2 curve for the current preferred value of Δm_s ¹⁷ (solid line). Right figure: Test of the goodness of the SM fit. The histogram (corresponding to the left scale) is the Monte Carlo-generated χ^2 distribution (see text), which is integrated to compute a CL, as given by the smooth curve (right scale). The χ^2 value of the current SM fit is indicated by the arrow, corresponding to a CL of 57%.

Parameter	95% CL region	Parameter	95% CL region
λ	0.2221 ± 0.0041	$ V_{ud} $	0.97504 ± 0.00094
A	0.76 - 0.90	$ V_{ub} [10^{-3}]$	3.15 - 4.37
$\bar{\rho}$	0.08 - 0.35	$ V_{cb} [10^{-3}]$	36.9 - 43.6
$\bar{\eta}$	0.28 - 0.45	$ V_{td} [10^{-3}]$	6.3 - 9.1
$J [10^{-5}]$	2.2 - 3.5	$ V_{ts} [10^{-3}]$	36.4 - 43.0
$\sin 2\alpha$	-0.81 - 0.43	$ V_{tb} $	0.99905 - 0.99932
$\sin 2\beta$	0.64 - 0.84	$\text{BR}(K_L^0 \rightarrow \pi^0 \nu \bar{\nu}) [10^{-11}]$	1.6 - 4.2
α	$77^\circ - 117^\circ$	$\text{BR}(K^+ \rightarrow \pi^+ \nu \bar{\nu}) [10^{-11}]$	5.1 - 8.4
β	$19.9^\circ - 28.6^\circ$	$\text{BR}(B^+ \rightarrow \tau^+ \nu_\tau) [10^{-5}]$	7.2 - 22.1
$\gamma = \delta_{CP}$	$40^\circ - 78^\circ$	$\text{BR}(B^+ \rightarrow \mu^+ \nu_\mu) [10^{-7}]$	2.9 - 8.7

Table 2: Fit results for the CKM parameters, the CKM matrix elements and branching ratios of some rare K and B meson decays, including the world average $\sin 2\beta$ in the fit. Ranges are given for the quantities that are limited by systematic theoretical errors.

One of these approaches, the QCD factorization approach (QCD FA)²², has been implemented in *CKMfitter*. The results obtained from these calculations are labelled by “R&D”, meaning that they are still subject to theoretical questions and that we do not intend to infer constraints on the CKM parameters from them. Rather, we intend to test the consistency of the QCD FA predictions in a global fit.

In the QCD FA, the tree, strong penguin and electroweak penguin amplitudes are computed, the annihilation diagrams estimated, and the soft physics contribution in the spectator interaction are parameterized. The strong phases are found to be small, and thus QCD FA predicts small direct CP asymmetries.

Global Fit of Branching Ratios and CP Asymmetries

In a first stage, a global fit on QCD FA is performed using the recent charmless two-body branching ratios (BR), given in table 3, and time-integrated CP asymmetries (A_{CP}), given in Table 4, as measured by the *BABAR*, *Belle* and *CLEO* collaborations²⁵.

The numerous theoretical parameters are free to vary in the global fit according to the

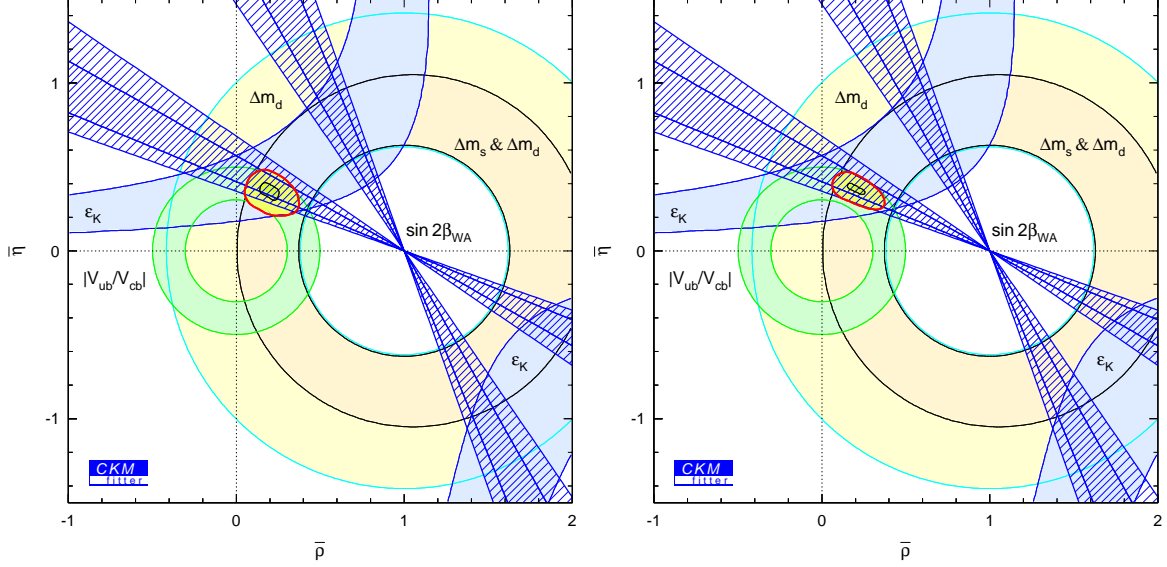


Figure 2: Constraints in the $\bar{\rho} - \bar{\eta}$ plane: regions with more than 5% CL are shown for the main observables: Δm_d , Δm_s , ϵ_K , $|V_{ub}/V_{cb}|$. The global SM fit constraint lies at the intersection of all individual measurements. For both the global fit and the new world average $\sin 2\beta$ constraint, two contour lines including points with more than 5% and 32% CL are drawn. Left plot: the $\sin 2\beta$ constraint is not included in the global SM fit, but is simply overlaid: the measurement is in perfect agreement with the SM expectation. Right plot: the $\sin 2\beta$ constraint is included in the global SM fit, and allows to pin down our knowledge on $\bar{\rho} - \bar{\eta}$.

Table 3: Branching ratios of the charmless two-body modes used in the global fit. The measurements from CLEO, BABAR and Belle collaborations²⁵ have been averaged into so-called World Average (WA) values.

BR ($\times 10^{-6}$)	CLEO (9.1 fb^{-1})	BABAR (55.6 fb^{-1})	Belle (31.7 fb^{-1})	WA
$B^0 \rightarrow \pi^+\pi^-$	$4.3_{-1.4}^{+1.6} \pm 0.5$	$5.4 \pm 0.7 \pm 0.4$	$5.1 \pm 1.1 \pm 0.4$	5.17 ± 0.62
$B^0 \rightarrow K^+\pi^-$	$17.2_{-1.4}^{+2.5} \pm 1.2$	$17.8 \pm 1.1 \pm 0.5$	$21.8 \pm 1.8 \pm 1.5$	18.5 ± 1.0
$B^0 \rightarrow K^+K^-$	$< 1.9(90\%)$	$< 2.5(90\%)$	$< 2.7(90\%)$	
$B^+ \rightarrow \pi^+\pi^0$	$5.6_{-2.3}^{+2.6} \pm 1.7$	$5.1 \pm 2.0 \pm 0.8$	$7.0 \pm 2.2 \pm 0.8$	5.9 ± 1.4
$B^+ \rightarrow K^+\pi^0$	$11.6_{-2.7-1.3}^{+3.0+1.4}$	$10.8 \pm 2.1 \pm 1.0$	$12.5 \pm 2.4 \pm 1.2$	$11.6_{-1.5}^{+1.6}$
$B^+ \rightarrow K^0\pi^+$	$18.2_{-4.0}^{+4.6} \pm 1.6$	$18.2 \pm 3.3 \pm 2.2$	$18.8 \pm 3.0 \pm 1.5$	$18.5_{-2.2}^{+2.3}$
$B^0 \rightarrow K^0\pi^0$	$14.6_{5.1-3.3}^{5.92.4}$	$8.2 \pm 3.1 \pm 1.2$	$7.7 \pm 3.2 \pm 1.6$	9.0 ± 2.2

predications of Ref. ²². In the left plot of Fig. 3, the QCD FA constraints from the charmless two-body BR and A_{CP} are compared to the SM constraints coming from all the measurements of Table 1.

One concludes that the QCD FA can accommodate the branching ratios and CP asymmetries of the $B \rightarrow \pi\pi$ and $B \rightarrow K\pi$ decays, and that the preferred value of the angle γ is around 80° . The constraints in the $\bar{\rho}-\bar{\eta}$ plane are in agreement with those obtained in the standard fit.

$C_{\pi\pi}$ and $S_{\pi\pi}$ Fits using QCD FA

The time-dependent CP asymmetry of $B^0 \rightarrow \pi^+\pi^-$ rate reads

$$a_{CP}(t) = S_{\pi\pi}\sin(\Delta m_d \Delta t) - C_{\pi\pi}\cos(\Delta m_d \Delta t), \quad (1)$$

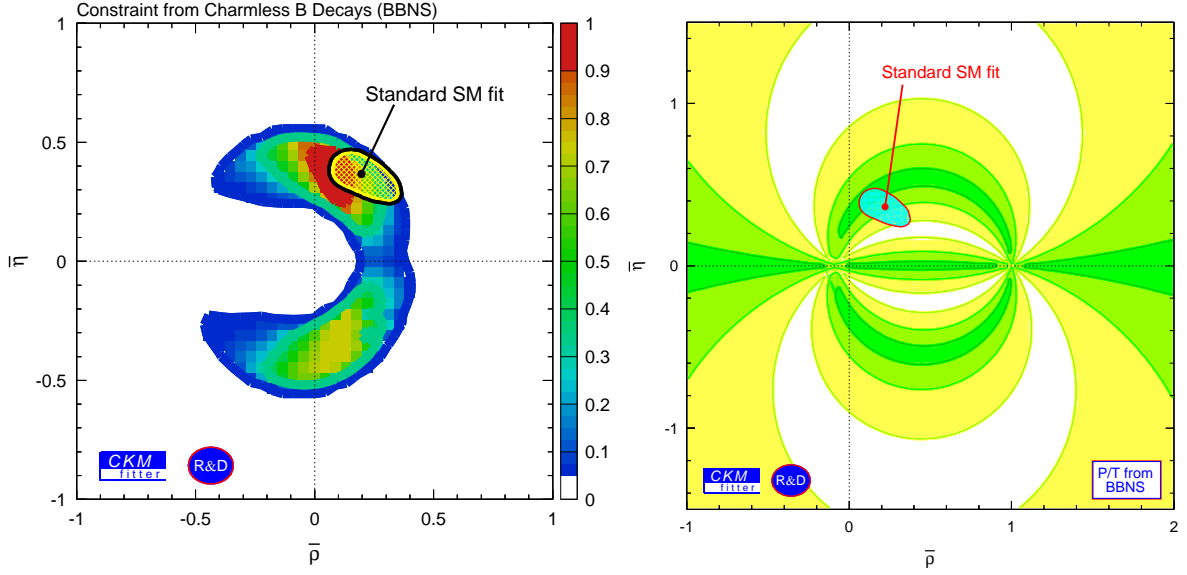


Figure 3: Left Plot: CL in the $(\bar{\rho} - \bar{\eta})$ plane obtained from a fit using branching ratios and CP asymmetries from Table 3, in the framework of the QCD FA approach. Right Plot: CL in the $(\bar{\rho} - \bar{\eta})$ plane obtained from a fit using $C_{\pi\pi}$ and $S_{\pi\pi}$ from *BABAR* where δ and the ratio $|P/T|$ are predicted by the QCD FA approach. The light, medium and dark shade zones include points with more than 5%,32%,90% CL.

Also shown is the 95% CL zone of the SM fit.

with Δt , the time difference between the CP and the tag B decays, and with the coefficients given by

$$S_{\pi\pi} = \frac{2\text{Im}\lambda_{\pi\pi}}{1 + |\lambda_{\pi\pi}|^2} \quad \text{and} \quad C_{\pi\pi} = \frac{1 - |\lambda_{\pi\pi}|^2}{1 + |\lambda_{\pi\pi}|^2}. \quad (2)$$

The CP parameter $\lambda_{\pi\pi}$ is given by

$$\lambda_{\pi\pi} = e^{-2i\beta} \frac{A(\bar{B}^0 \rightarrow \pi^+\pi^-)}{A(B^0 \rightarrow \pi^+\pi^-)} = e^{2i\alpha} \frac{1 - (R_t/R_u)|P/T|e^{-i(\alpha-\delta)}}{1 - (R_t/R_u)|P/T|e^{+i(\alpha+\delta)}} \equiv |\lambda_{\pi\pi}|e^{2i\alpha_{\text{eff}}}, \quad (3)$$

where the phase $e^{-2i\beta}$ arises from $B_d^0\bar{B}_d^0$ mixing, $R_{t(u)}$ are the sides of the UT⁸, and T, P are the tree and penguin amplitudes. In the presence of penguin contributions, the UT angle α enters the expression of $\lambda_{\pi\pi}$ with a correction term which depends, in particular, on the relative strong phase $\delta \equiv \arg(PT^*)$ between the penguin and the tree amplitudes. As a consequence, a measurement of the parameters $S_{\pi\pi}$ and $C_{\pi\pi}$ cannot be translated into $\sin 2\alpha$ without information on the relative strong phase δ and the ratio $|P/T|$, *e.g.*, as computed by the QCD FA approach.

The right plot in Fig. 3 and both plots in Fig. 4 show CL in the $\bar{\rho} - \bar{\eta}$ plane using the $C_{\pi\pi}$ and $S_{\pi\pi}$ measurements of *BABAR* and *Belle* respectively. While the *BABAR* measurement, interpreted within the QCD FA approach, is in good agreement with the SM expectations, the *Belle* measurement is in strong disagreement.

5 Beyond the Standard Model: the example of A_{SL}

Two classes of models beyond the SM have been investigated²⁶ using the semi-leptonic asymmetry which measures CP violation in B_d -mixing:

$$A_{\text{SL}} = \frac{\Gamma(\bar{B}^0(t) \rightarrow l^+ X) - \Gamma(B^0(t) \rightarrow l^- X)}{\Gamma(\bar{B}^0(t) \rightarrow l^+ X) + \Gamma(B^0(t) \rightarrow l^- X)} = \text{Im} \frac{\Gamma_{12}}{M_{12}}.$$

Table 4: Time-integrated direct CP asymmetries A in $B \rightarrow K\pi$ and CP parameters $C_{\pi\pi}$ and $S_{\pi\pi}$ ²⁵ of the time-dependent analysis in $B^0 \rightarrow \pi^+\pi^-$.

Observable	Value
$A_{CP}(B^0 \rightarrow K^+\pi^-)$	-0.05 ± 0.05 (WA)
$A_{CP}(B^+ \rightarrow K^+\pi^0)$	-0.09 ± 0.12 (WA)
$A_{CP}(B^+ \rightarrow K^0\pi^+)$	0.18 ± 0.10 (WA)
$S_{\pi\pi}$	-0.01 ± 0.38 (BABAR) $-1.21^{+0.41}_{-0.30}$ (Belle)
$C_{\pi\pi}$	-0.02 ± 0.30 (BABAR) $-0.94^{+0.32}_{-0.27}$ (Belle)

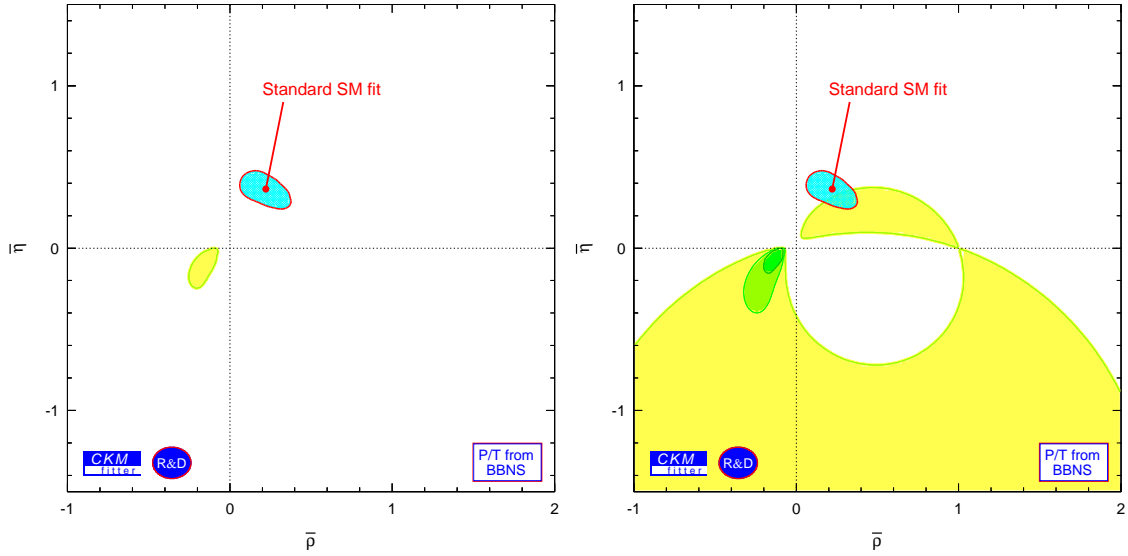


Figure 4: Left Plot: CL in the $\bar{\rho} - \bar{\eta}$ plane obtained from a fit using $C_{\pi\pi}$ and $S_{\pi\pi}$ from Belle, where the relative strong phase δ and the ratio $|P/T|$ are predicted by the QCD FA approach. The light, medium and dark shaded zones include points with more than 5%,32%,90% CL. Also shown is the 95% CL zone of the SM fit. Right Plot: zoom of the CL between 0 and 10%.

The present world-average²⁷ reads $A_{SL} = (0.2 \pm 1.4) \times 10^{-2}$. This parameter is predicted to be small (of the order of 10^{-3}) within the SM, but can be easily enhanced by new physics contributions.

In a class of models beyond the SM in which the CKM matrix is still a 3×3 unitary matrix and in which tree processes are dominated by the SM contributions (thus $\Gamma_{12} = \Gamma_{12}^{\text{SM}}$, and only M_{12} is affected by new physics), M_{12} can be parameterized by

$$M_{12} = r_d^2 e^{i2\theta_d} M_{12}^{\text{SM}}, \quad (4)$$

where r_d and θ_d are a modulus and a phase respectively. Constraints from $\sin 2\beta$, ΔM_d and A_{SL} are thus also modified.

The two left plots of Fig. 5 show CL in the $(r_d^2 - 2\theta_d)$ plane using all present constraints of the B_d meson system, including (middle plot) or not (left plot) the constraint from A_{SL} : one sees that the A_{SL} constraint disfavors the small r_d^2 and large $\sin 2\theta_d$ values.

A particular subset of the previous class of models have no new phase in flavour changing processes: these are the Minimal Favour Violating (MFV) models, as the minimal MSSM, the

two-Higgs doublets model, etc. In these models, one has:

$$r_d^2 = \frac{|F_{tt}|}{S_0(x_t)} \quad , \quad 2\theta_d = 0(\pi), \quad (5)$$

where $S_0(x_t)$ is the Inami-Lim function²⁸ depending on the top quark mass. F_{tt} enters ΔM_d , ΔM_s , ϵ_K , $\sin 2\beta$ and A_{SL} . The right plot of Fig. 5 shows CL in the $(\bar{\rho} - \bar{\eta})$ plane within the MFV framework, where negative values of $\bar{\eta}$ are no longer excluded^e. As can be seen through

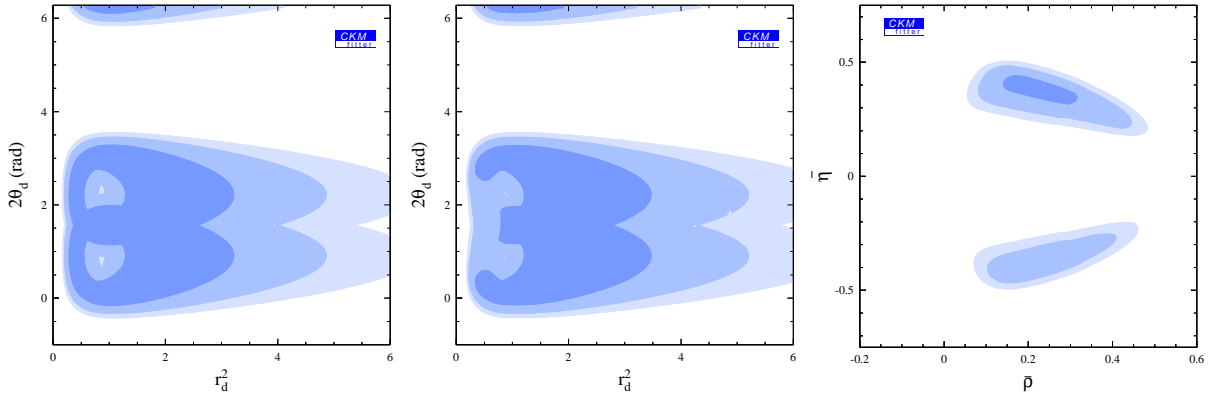


Figure 5: Left Plot: CL in the $r^2 - 2\theta_d$ plane using the present standard constraints of the B_d system. The light, medium and dark shaded zones corresponds to $CL > 10, 32$ and 90% respectively. Middle Plot: CL in the $r^2 - 2\theta_d$ plane using the standard constraints of the B_d system as well as the A_{SL} measurement. Right Plot: CL in the $\bar{\rho} - \bar{\eta}$ plane in the framework of the MFV models. Negative values of $\bar{\eta}$ are allowed.

the example of A_{SL} , a global CKM analysis is not only the place to test the Standard Model CKM paradigm, but also to investigate New Physics models, on which one can start to put meaningful constraints. When measurements reach a better precision, one will be able to rule out models, while favouring others.

6 Conclusion

The successful operation of the B factories at SLAC and KEK has provided a flood of new results that can be used to obtain information on the CP -violating phase of the CKM matrix. The extraordinary agreement of the world average of $\sin 2\beta$ with the indirect determination represents a new triumph for the Standard Model. It establishes the KM mechanism as the dominant source of CP violation in flavour changing processes at the electroweak scale. While the inclusion of $\sin 2\beta$ into the global CKM fit is a theoretically straightforward task, exploiting rare B decays requires some further theoretical understanding in order to lead to meaningful constraints at present.

Acknowledgements

Besides the one who was luckily present at the Moriond conference, four more persons are behind the *CKMfitter* group appellation and thus largely contributed to this presentation: A. Höcker, H. Lacker, F. Le Diberder, and J. Ocariz. I am indebted to all of them for such an enjoyable working atmosphere. I would like to thank as well the conference organizing committee for the invitation, the financial support, and the remarkable organization.

^eThis solution is highly dependent on the f_{B_d} value entering the ΔM_d prediction: it disappears for f_{B_d} larger than 210 MeV ²⁶.

References

1. J.H. Christenson, J.W. Cronin, V.L. Fitch, R. Turlay, *Phys. Rev. Lett.* **13**, 138 (1964)
2. B. Aubert *et al.*, BABAR Collaboration, *Phys. Rev. Lett.* **86**, 2515 (2001)
A. Abashian *et al.*, Belle Collaboration, *Phys. Rev. Lett.* **86**, 2509 (2001)
3. A.D. Sakharov, *JEPT Lett.* **6**, 21 (1967)
V.A. Kuzmin, V.A. Rubakov and M.E. Shaposhnikov, *Phys. Lett. B* **155**, 36 (1985)
K. Rummukainen *et al.*, *Nucl. Phys. B* **532**, 283 (1998)
4. Several groups have pioneered global CKM fits in the past. For the attempt of an exhaustive list, see Ref. [8]
5. N. Cabibbo, *Phys. Rev. Lett.* **10**, 351 (1963)
6. M. Kobayashi and T. Maskawa, *Prog. Theor. Phys* **49**, 652 (1973)
7. L. Wolfenstein, *Phys. Rev. Lett.* **51**, 1945 (1983)
We use the improved parameterization up to λ^6 proposed in A.J. Buras, M.E. Lautenbacher, G Ostermaier, *Phys. Rev. D* **50**, 3433 (1994)
8. A. Höcker, H. Lacker, S. Laplace and F. Le Diberder, *Eur.Phys.J C* **21**, 225 (2001)
Updates on <http://www.ckmfitter.in2p3.fr>
9. P. Harrison and H. Quinn (editors), The BaBar Physics Book, SLAC-R-504, 1998
10. M.H. Schune and S. Plaszczynski, talk given at 8th International Symposium on Heavy Flavor Physics, Southampton, England, 1999, *hep-ph/9911280*
11. M. Ciuchini *et al.*, JHEP 0107:013 (2001)
12. Vub LEP working group, <http://battagl.home.cern.ch/battagl/vub/vub.html>
13. B.H. Behrens *et al.*, CLEO Collaboration, *Phys. Rev. D* **61**, 052001 (2000)
14. A. Bornheim *et al.*, CLEO Collaboration, *hep-ex/0202019*
15. A. Höcker, H. Lacker, S. Laplace and F. Le Diberder, *hep-ph/0112295*
16. http://lepbose.web.cern.ch/LEPBOSC/combined_results/lathuile_2002
17. F. Le Diberder, <http://ckm-workshop.web.cern.ch/ckm-workshop>
18. S. Adler *et al.*, E787 Collaboration, *Phys. Rev. Lett.* **88**, 041803 (2002)
19. G. Buchalla and A. Buras, *Nucl. Phys. B* **398**, 285 (1993), *Nucl. Phys. B* **400**, 225 (1993), *Nucl. Phys. B* **548**, 309 (1999)
20. E949 web site: <http://www.phy.bnl.gov/e949>
21. Y. Keum, H. Li, A. Sanda, *Phys. Rev. D* **63**, 054008 (2001)
M. Ciuchini *et al.*, *Phys. Lett. B* **515**, 33-41 (2001)
22. M. Beneke, G. Buchalla, M. Neubert, C.T. Sachrajda, *Nucl. Phys. B* **606**, 245-321 (2001)
23. M. Bauer, B. Stech and M. Wirbel, *Z. Phys. C* **34**, 103 (1987)
24. J.D. Bjorken, *Nucl. Phys. B* **11**, 325 (1989)
25. A. Farbin, BABAR Collaboration, these proceedings.
B. Aubert *et al.*, BABAR Collaboration, *Phys. Rev. Lett.* **87**, 151802 (2001)
H. Lacker, CERN CKM Workshop (2002),
<http://ckm-workshop.web.cern.ch/ckm-workshop>
S. Chen *et al.*, CLEO Collaboration, *Phys. Rev. Lett.* **85**, 525-529 (2000)
D. Cronin-Hennessy *et al.*, CLEO Collaboration, *hep-ex/0001010*
26. S. Laplace, Z. Ligeti, Y. Nir and G. Perez, *Phys. Rev. D* **65**, 094040 (2002)
27. G. Abbiendi *et al.*, OPAL Collaboration, *Eur.Phys.J C* **12**, 609 (2000)
D.E. Jaffe *et al.*, CLEO Collaboration, *Phys. Rev. Lett.* **86**, 5000 (2001)
R. Barate *et al.*, ALEPH Collaboration, *Eur.Phys.J C* **20**, 431 (2001)
B. Aubert *et al.*, BABAR Collaboration, *Phys. Rev. Lett.* **88**, 231801 (2002)
28. T. Inami, C.S Lim, *Prog. Theor. Phys* **65**, 297 (1981)